EurJIC European Journal of Inorganic Chemistry

ChemPubSoc Europe

FULL PAPER

DOI:10.1002/ejic.201402089

Magnetic Study of a Pentanuclear $\{Co_2^{III}Co_3^{II}\}$ Cluster with a Bent $\{Co^{II}_3\}$ Motif

Irene C. Lazzarini,[a] Alejandro V. Funes,[a] Luca Carrella,[b] Lorenzo Sorace,[c] Eva Rentschler,[b] and Pablo Alborés*[a]

Keywords: Cluster compounds / Cobalt / Mixed-valent compounds / Magnetic properties / Density functional calculations / EPR spectroscopy

We have synthesised and structurally characterised a new pentanuclear mixed-valent cobalt cluster of formula $[Co^{II}_3Co^{III}_2(OH)_2(piv)_6(L)_2(H_2O)_4]$ (piv = trimethylacetate, H_2L = salicylideneanthranillic acid) from reaction of a dinuclear cobalt pivalate precursor with a Schiff base type ligand under mild reaction conditions. The core structure can be conveniently described as two fused Co_3–μ_3–OH triangles with a strict unique sharing vertex point. A complete picture of the magnetic behaviour of this compound is presented. Through combined use of susceptibility, magnetisation, and EPR data as well as broken-symmetry DFT calculations, we have supported the magnetic data that show weak and anisotropic exchange interaction between Co^{II} ions affording an S_{eff} = 1/2 ground state that is not completely isolated from the low-lying excited doublets at low temperature. Under the optimum applied field of 2 kOe, a frequency-dependent out-of-phase susceptibility signal can be observed below 4 K. However, no reliable relaxation rates could be extracted due to the narrow temperature range in which this behaviour was observed.

Introduction

Polynuclear transition-metal complexes bearing paramagnetic ions continue to attract much interest in the area of molecular magnetism, especially because they are good candidates for investigating slow relaxation of the magnetisation phenomena (single molecule magnet behaviour, SMM)[1] and, more recently, as promising units for molecular refrigerants[2] as well as in the field of molecular spintronics.[3]

A huge family of polynuclear complexes have been developed in which magnetic exchange interactions are mediated by oxygen-donor bridging ligands such as hydroxide, oxide, alkoxide and carboxylate ligands, or by a mixture of two or more ligands. In comparison with the well-extended and explored cluster chemistry of manganese and iron in different oxidation states[4] as 3d ions, the number of hydroxide- and/or carboxylate-bridged cobalt clusters for which the magnetic properties have been thoroughly investigated is still limited. This is probably due to the problems encountered when trying to gain a deeper understanding of their behaviour, largely as a result of the strong angular momentum appearing in the ground state at first order.[5] More recently, mirroring the development of single-ion-magnets (SIM) based on lanthanides,[6] examples based on mononuclear complexes containing 3d metal ions with unquenched orbital momentum have been reported,[7] some of them containing Co^{II} ions.[7c,7e,7f,7i] The driving force for this new approach is the possibility of exploiting the huge anisotropy of these systems, which produces a large barrier to magnetisation reorientation.

In the case of mixed-valence cobalt polynuclear complexes, because low-spin d^6 cobalt(III) is diamagnetic, the interesting magnetic properties arise from cobalt(II) alone, which is a paramagnetic ion with the possibility of exhibiting a strong Ising-type anisotropy.[5b,8] In this context, mixed-valency constitutes an alternative route to lower the Co^{II} content in cobalt polynuclear systems while preserving the molecular topology diversity. An efficient synthetic procedure, in the case of mixed valence clusters, consists of the slow oxidation of Co^{II} by air, in the presence of a carboxylate source and another auxiliary ligand with bridging ability.[9] One versatile ligand type in the preparation of high-nuclearity clusters are Schiff base derivatives of salycylaldehyde with amino-derivative groups. Following our research efforts in the field of polynuclear cobalt complexes,[9f,9i] we have explored a ligand (H_2L) from this family

[a] Departamento de Química Inorgánica, Analítica y Química Física/INQUIMAE (CONICET), Facultad de Ciencias Exactas y Naturales Universidad de Buenos Aires,
Pabellón 2, Ciudad Universitaria, C1428EHA Buenos Aires, Argentina
E-mail: albores@qi.fcen.uba.ar
http://www.inquimae.fcen.uba.ar/albores_pablo.htm
[b] Institute of Inorganic and Analytical Chemistry, Johannes Gutenberg University of Mainz,
Duesbergweg 10–14, 55128 Mainz, Germany
[c] Dipartimento di Chimica "U. Schiff" and UdR INSTM, Università di Firenze,
Via della Lastruccia 3, Polo Scientifico, 50019 Sesto Fiorentino, Firenze, Italy

Supporting information for this article is available on the WWW under http://dx.doi.org/10.1002/ejic.201402089.

© 2014 Wiley-VCH Verlag GmbH & Co. KGaA, Weinheim

using anthranillic acid (Scheme 1). The reaction of this ligand with a cobalt(II) pivalate (trimethyl acetate) precursor in the presence of a base, triethylamine, in acetonitrile afforded a new pentanuclear mixed-valent cobalt cluster of formula $[Co^{II}_3Co^{III}_2(OH)_2(piv)_6(L)_2(H_2O)_4]$ (piv = trimethylacetate). One hexanuclear $\{Zn_6\}$ compound[10] and a couple of dinuclear $\{Cu_2\}$ examples[11] are the only reported 3d metal complexes bearing this H_2L ligand, enhancing the relevance of this new $\{Co_5\}$ polynuclear compound.

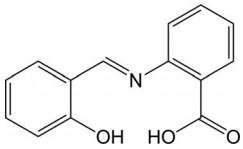

Scheme 1. Molecular representation of ligand H_2L employed in this work.

Herein, we report the structural characterisation of this new pentanuclear mixed-valent cobalt cluster and discuss in detail its magnetic behaviour. By considering the orbital contribution to the magnetic moment in the Co^{II} ions together with an anisotropic exchange interaction, we have been able to successfully explain macroscopic magnetisation and susceptibility data as well as the observed microscopic X-band EPR transitions.

Results and Discussion

Synthesis and Structural Characterisation

As we and others have previously shown, the starting cobalt(II) complex, $[Co_2(\mu\text{-}OH_2)(\mu\text{-}piv)_2(piv)_2(Hpiv)_4]$, can rearrange in solution to afford higher nuclearity cobalt compounds and, in this sense, it has proven to be a highly versatile synthetic precursor.[9f,9i,12] In the presence of the additional ligand H_2L and a suitable base (in this case, triethylamine), its reaction in an acetonitrile/methanol mixture at room temperature affords pentanuclear cobalt complex **1** in crystalline form, albeit in low yield.

We have found that the Co/H_2L ratio present in the reaction must be kept high to preclude isolation of mononuclear Co^{III} species with two L capping ligands. It was also found to be important to start the reaction in pure acetonitrile instead of methanol, because use of the latter afforded mixtures of lower nuclearity products. Because air was not excluded, this new compound exhibited a mixed valent $\{Co^{II}_3Co^{III}_2\}$ core, in which partial cobalt oxidation occurred, presumably by atmospheric oxygen.

Compound **1** crystallises in a monoclinic $P2_1/c$ cell. The asymmetric unit consists of one complex **1** moiety and two methanol solvent molecules. The molecular structure of **1** (Figure 1) is built up by five distorted octahedral cobalt ions held together by two $\kappa^1O\text{-}\mu_2\text{-}\kappa^1O'\kappa^1N$-(salicylidene)-anthranillate ligands, six μ_2-pivalates, and two μ_3-hydroxide ions. The remaining coordination sites completing all octahedral environments are occupied by four aqua ligands. The main bond angles and bond lengths are listed in the Supporting Information. Charge balance requires a $\{Co^{II}_3Co^{III}_2\}$ oxidation-state description, thus resulting in a mixed-valent complex. Cobalt–ligand distances fall into two well-separated groups, with distances involving Co(1) and Co(2) of 1.884–1.918 Å, and those from Co(3), Co(4) and Co(5) of 2.006–2.136 Å; thus, Co(1) and Co(2) are assigned as the Co^{III} ions. The inner core of the cluster (Figure 2) can be described as $[Co^{II}_3Co^{III}_2(\mu_3\text{-}OH)_2(\mu\text{-}OR)_2(\mu\text{-}OR')_6]^{2+}$, where R is the $\kappa^1O\text{-}\mu_2$-(salicylidene)anthranillate moiety and R′ corresponds to the μ_2-pivalate ligands. The cluster can be conveniently described as two fused $Co_3\text{–}\mu_3$-OH triangles with a strict unique sharing vertex point [at Co(3)] where both $\{Co_3\}$ triangles appear clearly twisted, making a Co(4)–Co(3)–Co(5) angle of 137.99(3) degrees. A pseudo C_2 axis runs along Co(3) and between both Co_3 triangle planes. Geometrical parameters describing both Co_3 units are listed in Table 1. To the best of our knowledge, there exist only two reported examples of this $[Co^{II}_3Co^{III}_2]$ motif, one with acetylacetonate and nitro ligands,[13] in which the Co^{II} sites make a considerably shorter angle of 99.3(1) degrees, and the second, a pivalate-based cluster with the $Co^{II}\text{–}Co^{II}\text{–}Co^{II}$ angle of 138.98(1) degrees,[12b] almost coincident with the value found in complex **1**.

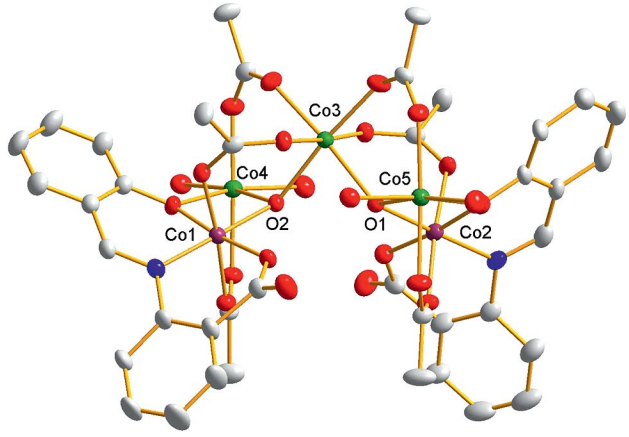

Figure 1. Molecular representation of compound **1**. *tert*-Butyl groups and H atoms have been omitted for clarity. Ellipsoids drawn at 30% probability level. Violet: Co^{III}, green: Co^{II}, red: O, blue: N, grey: C.

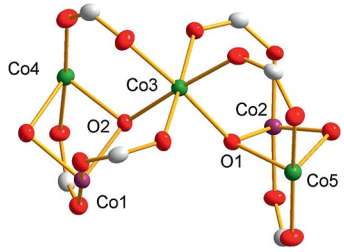

Figure 2. Molecular representation of the inner core in **1**, $[Co^{II}_3Co^{III}_2(\mu_3\text{-}OH)_2(\mu\text{-}OR)_2(\mu\text{-}OR')_6]^{2+}$, emphasising the two vertex-fused Co_3 triangles.

A rich intramolecular H-bond interaction network exists in addition to the intermolecular H-interactions (see the

 © 2014 Wiley-VCH Verlag GmbH & Co. KGaA, Weinheim

Table 1. Geometric parameters (Å, deg.) describing both vertex shared {Co^{II}_3-μ(OH)} units.

Co1–O2	1.908(4)
Co2–O1	1.917(4)
Co3–O1	2.103(4)
Co3–O2	2.112(4)
Co4–O2	2.091(4)
Co5–O1	2.087(4)
Co1–O3–Co4	98.35(19)
Co2–O4–Co5	96.7(2)
Co2–O1–Co5	96.13(18)
Co2–O1–Co3	122.8(2)
Co5–O1–Co3	120.4(2)
Co1–O2–Co4	97.27(19)
Co1–O2–Co3	122.2(2)
Co4–O2–Co3	119.2(2)

Supporting Information). Regarding the former, one of the two aqua ligands coordinated to Co(4) and Co(5), namely O(15) and O(23), are involved in H-interactions with the noncoordinating O atom of the L^{2-} ligand and a bridging pivalate. On the other hand, the O atoms of both μ_2-OH ligands, O(1) and O(2), show H-interactions with the μ_2O-atoms of L^{2-} ligands. With respect to the intermolecular interactions in the crystal packing, Co_5 molecules are arranged in chains strictly running along crystal *a*-axis. The chain arrangement relies on H-bond interactions between the O atoms of aqua and μ_2-pivalate ligands of neighbouring molecules (see the Supporting Information). The closest intermolecular Co···Co distance is 5.007(1) Å between Co(4) and Co(5)′. The chains are well-isolated among them [closest Co···Co distance between chains of 9.674(1)] through van der Waals type interactions involving the pivalate *tert*-butyl groups and L^{2-} phenyl rings. Methanol solvent molecules are not placed to fill voids but are located close to Co_5 moieties, with which they interact by forming hydrogen bonds, but they do not have any structural role in the intermolecular chain arrangement.

Magnetic Properties

Variable-temperature (2–300 K) DC magnetic susceptibility data at 0.1 kOe were recorded for **1** (Figure 3). The $\chi_m T$ product at 300 K of 12.5 $cm^3 mol^{-1} K$ is much higher than the spin-only value (g = 2.0) expected for three noninteracting S = 3/2 centres (5.62 $cm^3 mol^{-1} K$). This is clearly due to the orbital contribution of Co^{II}, which is known to be significant in an octahedral field.[8c] To achieve the observed $\chi_m T$ value at 300 K the g value must be close to 3, indicating that orbital contribution is not negligible. The continuous decrease in $\chi_m T$ with decreasing temperature may be due both to dominant antiferromagnetic interactions and/or to the depopulation of spin-orbit split levels arising from the $^4T_{1g}$ state in the octahedral field.[8c] On the other hand, dominant ferromagnetic interactions can be ruled out because a $\chi_m T$ increase should be observed at low T in this case, whereas $\chi_m T$ monotonically decrease reaching a value of 2.31 $cm^3 mol^{-1} K$ at 2 K.

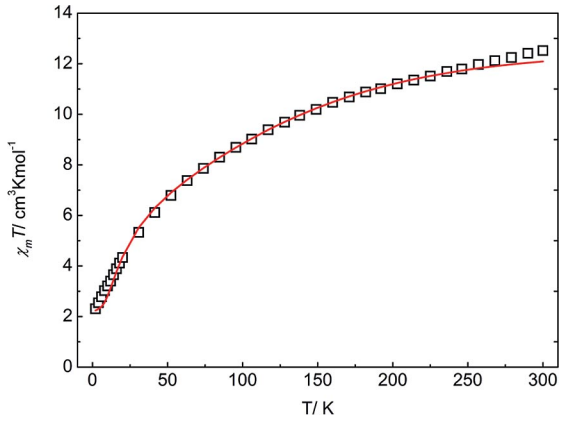

Figure 3. $\chi_m T$ vs. T data plot at 1 kOe in the 2–300 K range for compound **1**. Squares: experimental; Full line: fitted (see text).

Inspection of the Co_5 cluster magnetic interaction topology reveals an angular trinuclear Co^{II} arrangement (because low spin d^6 Co^{III} ions are diamagnetic) with only two possible distinct exchange interactions, if present (Figure 4). This topology definitely excludes any possibility of competing exchange interactions, as would be expected in the case of a triangular arrangement.

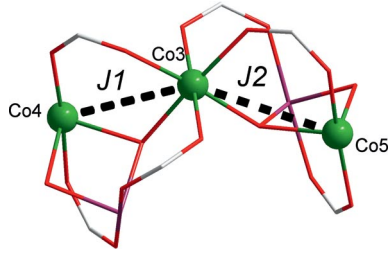

Figure 4. Possible Co^{II}–Co^{II} exchange interactions in compound **1**.

Magnetisation data recorded at different applied external fields (1–70 kOe) in the 2–10 K temperature range further proves a magnetic ground state (Figure 5). Magnetisation sharply increases upon cooling the sample to 2 K and sweeping field up to 70 kOe. Clear saturation was observed in the reduced magnetisation plots at highest achievable field and lowest temperature, with a value of 3.5$N\beta$. No superposition of the isofield lines was observed, suggesting the existence of anisotropy or low-lying multiplets above the spin ground state.

Our general approach to fit the magnetic data was based on determining the energy of the different spin states through diagonalisation of the corresponding Hamiltonian and calculating the molar magnetisation for all possible field (H) orientations (θ) with the following equation:

$$M(\vartheta,H)=\frac{N\sum_n\left(-\partial E_i(\vartheta,H)/\partial H\right)\exp\left(-E_i(\vartheta,H)/kT\right)}{\sum_i\exp\left(-E_i(\vartheta,H)/kT\right)} \quad (1)$$

© 2014 Wiley-VCH Verlag GmbH & Co. KGaA, Weinheim

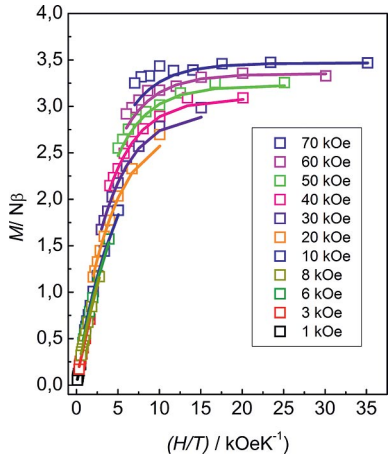

Figure 5. M vs. H/T data plot in the range 0–70 kOe and 2–10 K of compound **1**. Squares: experimental; Full line: fitted (see text).

The susceptibility was then calculated as the ratio between M and H. Although it is possible to make a reasonable fitting with a spin-only Hamiltonian considering the exchange interaction between three S = 3/2 ions, the extremely high g value (above 3) obtained in this way suggests that orbital contribution is strong and cannot be ignored. Hence, to analyse susceptibility data in the whole temperature range, the following Hamiltonian must be preferentially employed:

$$\hat{H} = \beta H\left(-\frac{3}{2}\kappa\lambda\sum_{i=1-3}\hat{L}_i + (g_0+\Delta g)\sum_{i=1-3}\hat{S}_i\right) - \frac{3}{2}\kappa\lambda\sum_{i=1-3}\hat{L}_i\hat{S}_i - V_{ax}\sum_{i=1-3}\left(\hat{L}_{i,z}^2 - \frac{2}{3}\right) - 2J_{exc}(\hat{S}_1\hat{S}_2 + \hat{S}_1\hat{S}_3) \quad (2)$$

where the orbital component is expressed in terms of the P term (L = 1) isomorphous with the T_{1g} term and κ is the reduction factor taking into account covalency and mixing of the $^4T_{1g}$ terms (from ground ^4P and excited ^4F terms), and λ is the spin-orbit coupling constant.[5b,8c] The g_0 factor equals the g_e value if mixing with excited states other than $^4T_{1g}$ is neglected: however, the contribution of excited states can shift the g_0 factor by a sizeable Δg magnitude.[5b] V_{ax} accounts for possible distortions from pure octahedral symmetry, and the last term reflects the exchange interaction term operating only over the S components following Lines model.[14] To minimise over-parameterisation, all Co^{II} sites have been forced to share a unique set of parameters, Δg, κ, λ and V_{ax}. For the same reason, a unique exchange coupling constant should be included in spite of the strict existence of two different Co^{II} interacting pairs. An initial attempt to fit $\chi_m T$ data in the whole 2–300 K range excluding the exchange interaction term (J_{exc} = 0) failed. Only data above ca. 100 K could be reasonably reproduced, with large uncertainty towards the axial distortion parameter (see the Supporting Information). This result can be taken as the first evidence for the existence of exchange interaction between Co^{II} ions, of antiferromagnetic nature due to negative $\chi_m T$ data deviation from best-fit plot. Moreover, when considering a three exchanged S = 3/2 system, the 100 K limit provides a first approximation of the magnitude of the J_{exc} parameter of about –4 cm^{-1} (with this magnitude all spin multiplet levels become equally populated above ca. 100 K). At this point of analysis, it should also be remarked that weak intermolecular interactions may influence the final value found for the J_{exc} parameter, which can be inferred from structural data. However, the expected value for this type of exchange interaction is normally an order of magnitude lower.

Once the exchange interaction term was included, a $\chi_m T$ data fitting in the whole 2–300 K range (Figure 3) afforded the parameters: J_{exc} = –3.2 ± 0.3 cm^{-1} and Δg = 0.34 ± 0.02 ($R = 6.19 \times 10^{-4}$). The κ and λ parameters were fixed at typical and reasonable values of 1 and –180 cm^{-1} to avoid over-parametrisation. As previously shown, it was not possible to obtain a reliable magnitude for the axial distortion term, thus it was not included in the fitting procedure. However, it is clear that local symmetry around the Co^{II} sites deviate from an octahedral symmetry when considering structural data [CShM 0.226, 0.757 and 0.895 for Co(3), Co(4) and Co(5) respectively, calculated with SHAPE[15] for the octahedron reference polyhedra], however, the individual site distortion parameters cannot be extracted from the average powder susceptibility data as just argued.

It is possible, alternatively, to analyse the low-temperature data considering the three Co^{II} centres as effective S_{eff} = 1/2 coupled through an effective exchange interaction term.[5b,8b,9e] This approach relies on the fact that at low enough temperature (below ca. 30 K) only the lowest Kramers doublet, arising from the $^4T_{1g}$ ground state term after spin-orbit interaction and low-symmetry distortion, is populated. In this way, the number of parameters becomes considerably reduced. Magnetisation data naturally appears as the best target to test this effective spin approach.

At the limit of a large antiferromagnetic exchange interaction, a S_{eff} = 1/2 ground state should only be populated and magnetisation data must follow a Brillouin behaviour.[16] This is not the case and, as this ground doublet cannot be split at zero field, it becomes evident that the observed magnetisation profile is due to low-lying excited states (hence a small but not negligible exchange interaction parameter, as suggested from susceptibility data) or anisotropy arising from the exchange interaction (anisotropic exchange interaction contributions). Attempts to fit data with an isotropic effective exchange interaction Hamiltonian were completely unsuccessful. It is well-known that the lowest Co^{II} ion Kramers doublet can be highly anisotropic due to the strong orbital momentum contribution leading to anisotropic g^{eff} factors and anisotropic J^{eff}.[8a,8b] To consider this anisotropic behaviour, the following general Hamiltonian can be employed:

$$\hat{H} = -2J_z^{eff}(\hat{S}_{1z}^{eff}\hat{S}_{2z}^{eff} + \hat{S}_{2z}^{eff}\hat{S}_{3z}^{eff} + \alpha_x(\hat{S}_{1x}^{eff}\hat{S}_{2x}^{eff} + \hat{S}_{2x}^{eff}\hat{S}_{3x}^{eff}) + \alpha_y(\hat{S}_{1y}^{eff}\hat{S}_{2y}^{eff} + \hat{S}_{2y}^{eff}\hat{S}_{3y}^{eff})) + \beta\sum_{i=1-3}\left(g_{x,i}^{eff}\hat{S}_{x,i}^{eff}H_x + g_{y,i}^{eff}\hat{S}_{y,i}^{eff}H_y + g_{z,i}^{eff}\hat{S}_{z,i}^{eff}H_z\right) \quad (3)$$

where $J_{x,y}^{eff} = \alpha_{x,y}J_z^{eff}$ and again a unique exchange interaction as well as an average isotropic g^{eff} (it is clear that this is not a particularly realistic assumption but is necessary at

 © 2014 Wiley-VCH Verlag GmbH & Co. KGaA, Weinheim

this stage) can only be employed to prevent severe overparametrisation. Even with these assumptions, a high degree of correlation between fitting parameters is found. To obtain more reliable values, a number of additional restraints must be applied.

The isotropic effective exchange coupling constant, $J_{iso}^{eff} = (J_x + J_y + J_z)/3$, is approximately related to the J_{exc} operating over the $S = 3/2$ system at first order, by the following relationship:

$$J_{iso}^{eff} = \frac{25}{9} J_{exc} \quad (4)$$

From this expression and the obtained magnitude of the isotropic exchange parameter from susceptibility data, a value for J_{iso}^{eff} close to –8 cm^{-1} should be expected. This allows a set of best fitting parameters to be isolated for the M vs. H data employing the Hamiltonian of Equation (3), $g_{eff} = 4.2 \pm 0.6$; $J_{iso}^{eff} = -8$ cm^{-1} (fixed); $a_x = -1.1 \pm 0.2$; $a_y = -0.5 \pm 0.4$ ($R = 8.9 \times 10^{-4}$) (Figure 5).

With the aim of further testing the whole set of parameters describing magnetic data, we performed powder X-band EPR (9.403 GHz) measurements of compound **1** at 5 and 20 K (Figure 6 and the Supporting Information). The spectra resembles a $S_{eff} = 1/2$ with clear axial anisotropy, with broad resonances at ca. 500 and 1300 Oe and even weaker and broader features at higher fields. The approximate g^{eff} values corresponding to resonance fields are $g_z^{eff} \approx 13.4$ and $g_{xy}^{eff} \approx 5.2$. These values are clearly out of the expected range for a single Co^{II} ion[17] further proving, independently from susceptibility and magnetisation data, the existence of exchange interaction. Employing the Hamiltonian of Equation (3) with a minimum parameter's set (two different g-tensors and a unique anisotropic exchange interaction matrix) allows the main features of the EPR spectra to be simulated (Figure 6). When running spectra simulations applying restraints to simultaneously fit magnetisation data, the following parameters were obtained, which reasonably reproduce EPR spectra: $g_{1x,y,z} = \{0.4, 3.5, 7.5\}$; $g_{2x,y,z} = \{0, 0, 8.3\}$; $J_{exc}^{iso} = -8$ cm^{-1} (fixed); $a_x = -1.0$; $a_y = -0.7$. Rhombicity of g^{eff} is necessary to properly simulate the intensity ratio between low-field and high-field transitions, which cannot be simulated with a pure axial g^{eff}.

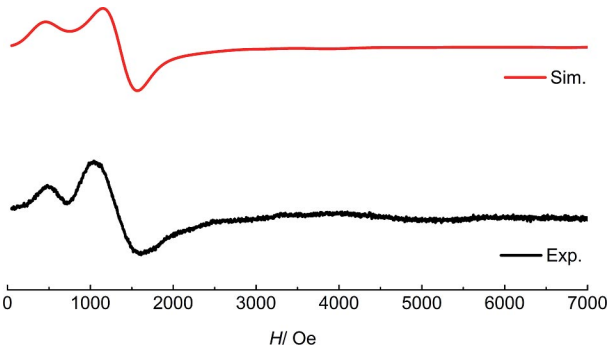

Figure 6. EPR spectra (X-band; 9.403 GHz) of a powder of **1** at 5 K. Simulation line width: 380 Oe.

It was not possible to obtain good simulations by employing either a common g-tensor or an isotropic exchange interaction term. When keeping magnetisation and susceptibility data in agreement with EPR spectra this consistent set of parameters was found. Similar anisotropic g-tensor values have been observed or calculated in other six-coordinate Co^{II} systems.[9d,9e,9o,18] Naturally, a similar EPR simulation can be performed with an isolated $S_{eff} = 1/2$ model (however in this way it is not possible to link the results with magnetisation and susceptibility data as a whole) and an effective anisotropic g-tensor: $g_{x,y,z}^{eff} = \{0.4, 5.0, 14.8\}$.

It must be noted that this is a quite simplified picture of the system (for example, nothing can be said about either the relative main g-tensor axis orientation or about the two different Co–Co exchange interactions and local distortion terms) but it is enough to support the existence of anisotropic exchange interaction between highly anisotropic $S_{eff} = 1/2$ sites with an overall isotropic antiferromagnetic interaction component.

To test for possible slow magnetisation relaxation behaviour, alternating-current (AC) magnetic susceptibility of **1** was investigated under zero and nonzero applied static fields, respectively (see the Supporting Information). Although no peaks of χ_m'' were observed under zero DC magnetic field, even at the highest achievable frequency ($\nu = 1500$ Hz), nonzero χ_m'' signals appeared when a static DC field (2 kOe) was applied, suggesting the onset of a slow relaxation of the magnetic moment. However, at the highest available frequency and lowest temperature, no maximum in the temperature dependence profile could be distinguished, precluding characteristic relaxation time data extraction and any further information on the relaxation mechanism.

DFT Calculations

To gain deeper insight into the origin of the isotropic antiferromagnetic component of the exchange interaction between the Co^{II} ions in compound **1**, we performed broken-symmetry DFT calculations to evaluate the magnitude of the exchange coupling constants employing the hybrid B3LYP functional and a valence core big size (TZP) basis set. This approach has previously been successful when applied to closely related systems.[9i,12a,19] It must be clearly stated that these calculated exchange coupling constant values correspond to $S = 3/2$ interacting Co^{II} under a complete spin-only isotropic HDvV model, which does not directly compare with experimental data extracted through the $S_{eff} = 1/2$ modelling. However, it is still useful to obtain an indication of the order of magnitude and the sign of the exchange interactions as well as possible magnetic orbital exchange pathways involved.

The calculations allow, in principle, different values for both J_1 and J_2 coupling constants to be obtained (Figure 4), whereas it was not possible to delineate these values exclusively from experimental data. Because the exchange interaction between both apical Co^{II} sites was neglected,

 © 2014 Wiley-VCH Verlag GmbH & Co. KGaA, Weinheim

only two from the three possible combination of broken-symmetry spin state energies become useful for exchange coupling constant calculation: those that combine BS1–BS2 and BS1–BS3. This is due to an important degree of correlation found between both exchange pathways, as can be inferred from an inspection of magnetic COT orbitals arising from the BS2 and BS3 states (see the Supporting Information) where no clean unique Co–Co interaction pair can be distinguished. In fact, the obtained values are: J_1 = –3.8 cm^{-1}; J_2 = –4.4 cm^{-1} for the former combination and J_1 = –37 cm^{-1}; J_2 = 29 cm^{-1} in the case of the latter combination, leaving uncertainty about the sign of both exchange interactions. However, when considering the key BS1 state, the following J_1 – J_2 relationship is obtained: J_1 + J_2 = –8.3 cm^{-1}, which is in excellent agreement with experimental observation.

To better understand the results described above, it is useful to analyse the key structural features governing the exchange pathways as well as the magnetic orbitals involved. Both exchange interactions are similarly mediated by μ_2-OH and μ_2-(*syn-anti*)-carboxylate bridges with small differences in bond lengths and bond angles. Particularly, the critical Co–O–Co angle involving the hydroxide bridge is almost identical and close to 120°, favouring magnetic orbital overlaps, all of them of mixed π-σ type, as can be observed in the COT representation arising from the BS1 state (Figure 7). Most of the previously reported Co^{II} polynuclear complexes with related bridging ligands such as alkoxide, hydroxide, oxo and aqua, showing ferromagnetic interactions, have Co–O–Co angles well below 100°.[9i,20] Due to the usual complexity of local symmetry over Co^{II} sites in these systems it is not straightforward to convincingly rationalise these magnetostructural aspects and there is still no clear picture emerging to solve this problem.

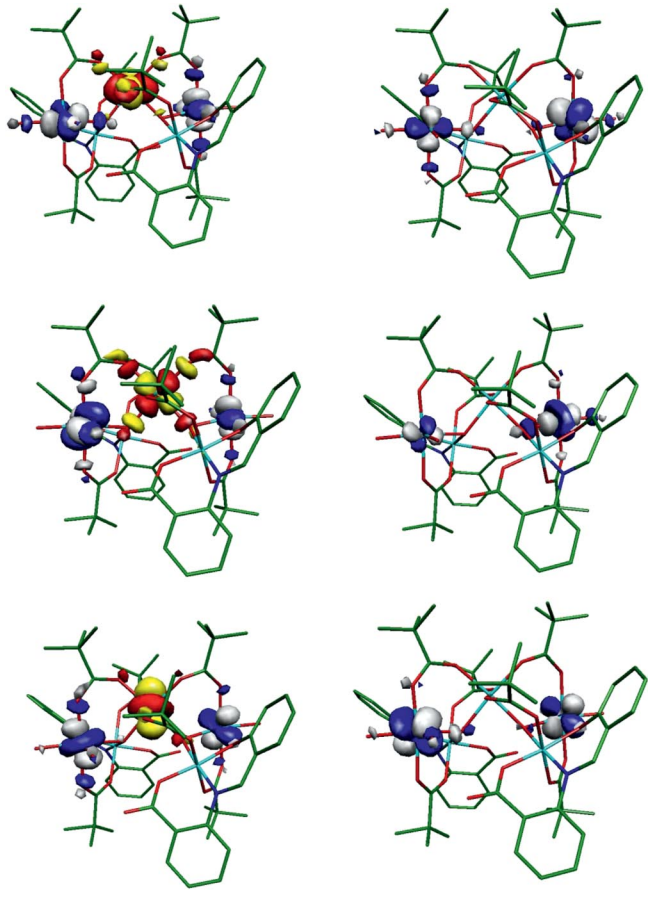

Figure 7. Magnetic orbitals after a COT arising from the BS1 state showing possible exchange pathways. Alpha orbitals: blue/white; Beta orbitals: red/yellow. Isosurface value: 0.03 a.u.

More specifically, among the narrow group of reported mixed-valent {Co$^{II}_3$Co$^{III}_2$} clusters[12b,13,20c,20d] it is difficult to find examples with extensively analysed magnetic data. The related {Co$^{II}_3$Co$^{III}_2$} compounds sharing strictly the same {Co$^{II}_3$} topology lack detailed magnetic studies,[12b,13] as well as, to the best of our knowledge, the trinuclear Co^{II} compound with exactly the same motif.[21]

Conclusions

We have given a complete picture of the magnetic behaviour of a novel pentanuclear mixed-valent cobalt cluster bearing a bent μ_2-hydroxide–μ_2-carboxylate bridged {Co$^{II}_3$} motif. By the combined use of susceptibility, magnetisation, and EPR data, as well as broken-symmetry DFT calculations, we have supported a magnetic data interpretation that shows weak and anisotropic exchange interaction between Co^{II} ions affording an S_{eff} = 1/2 ground state that is not completely isolated from the low-lying excited doublets at low temperature, as evidenced from magnetisation data plots. Interestingly, under the optimum applied field of 2 kOe, a frequency-dependent out-of-phase susceptibility signal can be observed below 4 K. However, no relaxation rates can be reliably extracted and no indication as to the relaxation mechanism can be obtained, due to the narrow temperature and frequency range over which this behaviour is observed. In single Co^{II} systems, even those with positive ZFS *D* parameters, relatively large thermal barriers for magnetisation reversal have recently been observed.[7e,7f] These systems are described by an energy level pattern mainly composed of Kramers doublets, with lowest m_S projection as the ground state. A similar picture arises in the case of **1**, however, in this case, fast tunnelling must be preventing the observation of slow magnetisation relaxation at higher temperatures. To better understand the factors governing this behaviour, more examples with this {Co$^{II}_3$} topology must be generated, which can be achieved by exploring different auxiliary ligands; studies in this direction are ongoing in this research programme.

Experimental Section

Material and Physical Measurements: [Co$_2$(μ-OH$_2$)(μ-piv)$_2$(piv)$_2$(Hpiv)$_4$], piv = trimethylacetate, was prepared by following a reported procedure.[12b] The Schiff base ligand employed in this work was prepared by using a standard procedure: equimolar amounts of salycylaldehyde and anthranillic acid were mixed and heated to reflux in ethanol and crystallised as orange needles upon cooling

© 2014 Wiley-VCH Verlag GmbH & Co. KGaA, Weinheim

to room temperature. All other chemicals were reagent grade and used as receive without further purification. Elemental analysis was performed with a Carlo Erba 1108 analyser.

$[Co^{II}_3Co^{III}_2(OH)_2(piv)_6(L)_2(H_2O)_4]\cdot 2H_2O$ (1): Dinuclear precursor $[Co_2(\mu\text{-}OH_2)(\mu\text{-}piv)_2(piv)_2(Hpiv)_4]$ (0.2 g, 0.2 mmol) was dissolved in acetonitrile (20 mL) at room temperature. To this solution, H_2L (0.05 g, 0.2 mmol; H_2L = salicylideneanthranillic acid) and triethylamine (0.042 g, 0.4 mmol), dissolved in acetonitrile (15 mL), were added under vigorous stirring. The resulting solution immediately turned dark-red. After stirring for 1 h, the solution was left undisturbed at room temperature. After one week, yellow needles crystallised. At this point, methanol (15 mL) was added and the needles redissolved. The resulting solution was again left to slowly evaporate. After six further weeks, dark-red block-shaped crystals of **1** appeared, which were collected by filtration, washed with acetonitrile and air dried, yield 10 mg (8%; Co based). $C_{58}H_{86}Co_5N_2O_{26}$ (1521.97): calcd. C 45.8, H 5.7, N 1.8; found C 45.4, H 5.7, N 2.0.

Magnetic Measurements: Magnetic measurements were performed with a Quantum Design MPMS-XL-7 SQUID magnetometer. All experimental magnetic data were corrected for the diamagnetism of the sample holders and of the constituent atoms (Pascal's tables). AC measurements were performed at driving frequencies ranging 10 to 1400 Hz with AC field amplitude of 3 Oe in DC fields ranging 0–30 kOe. X-Band EPR spectra were measured with a Bruker Elexsys E500 spectrometer equipped with a liquid ^{4}He flux cryostat (ESR900, Oxford Instruments) to measure at low temperatures. Spectra were simulated with the Easyspin package.[22]

X-ray Structure Determination: The crystal structure of **1** was determined with an Oxford Xcalibur, Eos, Gemini CCD area-detector diffractometer using graphite-monochromated Mo-K_α radiation (λ = 0.71069 Å) at 298 K. Data was corrected for absorption with CrysAlisPro, Oxford Diffraction Ltd., Version 1.171.33.66, applying an empirical absorption correction using spherical harmonics, implemented in SCALE3 ABSPACK scaling algorithm.[23] The structure was solved by direct methods with SHELXS-97[24] and refined by full-matrix least-squares on F^2 with SHELXL-97.[24] Hydrogen atoms were added geometrically and refined as riding atoms with a uniform value of U_{iso}. Hydrogen atoms of hydroxide and water coordinated molecules were located in the Fourier difference map and subsequently refined. *tert*-Butyl groups in five of the six pivalate ligands were found disordered over two distinct positions and were refined as two disordered groups with fixed 0.5:0.5 occupancy ratio. One of the two methanol solvent molecules was also found disordered and was thus isotropically refined over two split positions with 0.5:0.5 fixed occupancy ratio. Final crystallographic data and values of R_1 and wR are listed in Table S1 (see the Supporting Information), and the main angles and distances are listed in Table S2 (see the Supporting Information). CCDC-977362 contains the supplementary crystallographic data for this paper. These data can be obtained free of charge from the Cambridge Crystallographic Data Centre via www.ccdc.cam.ac.uk/data_request/cif.

Quantum Chemical Calculations: Density functional theory (DFT) spin-unrestricted calculations were performed by using the ADF 2010.02 program[25] at the B3LYP level employing a frozen core TZP basis. High accuracy converged (less than 1e^{-6} Hartrees in the commutator of the Fock and the P-matrices) single point calculations at the X-ray geometries were performed to analyse the exchange coupling between cobalt centres. The methodology applied here relies on the broken symmetry formalism, originally developed by Noodleman for SCF methods, which involves a variational treatment within the restrictions of a single spin-unrestricted Slater determinant built upon using different orbitals for different spin.[26] This approach has later been applied within the frame of DFT.[27] The HS (high spin) and BS (broken symmetry) energies were then combined to estimate the exchange coupling parameter J involved in the widespread used Heisenberg–Dirac–van Vleck Hamiltonian. We have calculated the different spin topologies of broken symmetry nature (see the Supporting Information) by alternately flipping spin on the different metal sites. The exchange coupling constants J_i can be obtained by considering the individual pair-like components spin interactions involved in the description of the different broken symmetry states. We used the method proposed by Ruiz and co-workers,[28] where the following equation is applied:

$$E_{BS} - E_{HS} = 2J_{12}(2S_1S_2 + S_2), \text{ with } S_2 < S_1$$

In both cases, a set of linear equations must be solved to obtain the J parameters. Additionally, we have also employed a corresponding orbital transformation, COT over the BS solutions,[29] as a means to visualise the magnetic orbitals and the involved spin-coupling exchange pathways between alpha and beta COs.

Supporting Information (see footnote on the first page of this article): Crystallographic data of **1**, X-band EPR spectra of **1** at 20 K, χ_mT vs. T plots of **1**, plots of χ_m'' vs H for **1**, spin density maps, magnetic orbitals.

Acknowledgments

The authors gratefully acknowledge Universidad de Buenos Aires (UBA), Agencia Nacional de Promoción Científica y Tecnológica (ANPCYT) and Consejo Nacional de Investigaciones Científicas y Técnicas (CONICET) for funding resources. P. A. is a staff member of CONICET and A. V. F. is a doctoral fellow of CONICET. DFT computations were performed at the Jülich Supercomputer Center (JSC), Germany, under the NIC project 4953.

[1] a) G. Christou, D. Gatteschi, D. N. Hendrickson, R. Sessoli, *MRS Bull.* **2000**, *25*, 66; b) G. Aromi, E. K. Brechin, in: *Single-Molecule Magnets and Related Phenomena* (Ed.: R. Winpenny), **2006**, *vol. 122*, p. 1–67; c) D. Gatteschi, R. Sessoli, J. Villain, *Molecular Nanomagnets*, Oxford University Press, **2006**.

[2] a) Y.-Z. Zheng, G.-J. Zhou, Z. Zheng, R. E. P. Winpenny, *Chem. Soc. Rev.* **2013**, *43*, 1462–1475; b) R. Sessoli, *Angew. Chem. Int. Ed.* **2012**, *51*, 43; *Angew. Chem.* **2012**, *124*, 43; c) M. Evangelisti, E. K. Brechin, *Dalton Trans.* **2010**, 4672.

[3] a) L. Bogani, W. Wersndorfer, *Nat. Mater.* **2008**, *7*, 179; b) S. Sanvito, *Chem. Soc. Rev.* **2011**, *40*, 3336.

[4] a) T. C. Stamatatos, G. Christou, *Philos. Trans. R. Soc. London Ser. A* **2008**, *366*, 113; b) D. Gatteschi, A. Caneschi, R. Sessoli, A. Cornia, *Chem. Soc. Rev.* **1996**, *25*, 101; c) A. M. Ako, O. Waldmann, V. Mereacre, F. Klower, I. J. Hewitt, C. E. Anson, H. U. Gudel, A. K. Powell, *Inorg. Chem.* **2007**, *46*, 756; d) A. M. Ako, V. Mereacre, Y. Lan, W. Wersndorfer, R. Cl, C. E. Anson, A. K. Powell, *Inorg. Chem.* **2009**, *48*, 1; e) A. A. H. Abu-Nawwas, P. V. Mason, V. A. Milway, C. A. Muryn, R. J. Pritchard, F. Tuna, D. Collison, R. E. P. Winpenny, *Dalton Trans.* **2008**, *198*; f) A. A. Smith, R. A. Coxall, A. Harrison, M. Helliwell, S. Parsons, R. E. P. Winpenny, *Polyhedron* **2004**, *23*, 1557.

[5] a) G. E. Kostakis, S. P. Perlepes, V. A. Blatov, D. M. Proserpio, A. K. Powell, *Coord. Chem. Rev.* **2012**, *256*, 1246; b) S. Ostrovsky, Z. Tomkowicz, W. Haase, *Coord. Chem. Rev.* **2009**, *253*, 2363.

[6] a) N. Ishikawa, M. Sugita, T. Ishikawa, S. Koshihara, Y. Kaizu, *J. Am. Chem. Soc.* **2003**, *125*, 8694; b) D. N. Woodruff, R. E. P. Winpenny, R. Layfield, *Chem. Rev.* **2013**, *113*, 5110; c) L. Sorace, C. Benelli, D. Gatteschi, *Chem. Soc. Rev.* **2011**, *40*, 3092; d) J. D. Rinehart, J. R. Long, *Chem. Sci.* **2011**, *2*, 2078.

 © 2014 Wiley-VCH Verlag GmbH & Co. KGaA, Weinheim

[7] a) D. E. Freedman, W. H. Harman, T. D. Harris, G. J. Long, C. J. Chang, J. R. Long, *J. Am. Chem. Soc.* **2010**, *132*, 1224; b) W. H. Harman, T. D. Harris, D. E. Freedman, H. Fong, A. Chang, J. D. Rinehart, A. Ozarowski, M. T. Sougrati, F. Grandjean, G. J. Long, J. R. Long, C. J. Chang, *J. Am. Chem. Soc.* **2010**, *132*, 18115; c) J. M. Zadrozny, J. R. Long, *J. Am. Chem. Soc.* **2011**, *133*, 20732; d) S. Mossin, B. L. Tran, D. Adhikari, M. Pink, F. W. Heinemann, J. Sutter, R. K. Szilagyi, K. Meyer, D. J. Mindiola, *J. Am. Chem. Soc.* **2012**, *134*, 13651; e) J. M. Zadrozny, J. Liu, N. a. Piro, C. J. Chang, S. Hill, J. R. Long, *Chem. Commun.* **2012**, *48*, 3927; f) E. Colacio, J. Ruiz, E. Ruiz, E. Cremades, J. Krzystek, S. Carretta, J. Cano, T. Guidi, W. Wersndorfer, E. K. Brechin, *Angew. Chem. Int. Ed.* **2013**, *52*, 9130; g) J. M. Zadrozny, D. J. Xiao, M. Atanasov, G. J. Long, F. Grandjean, F. Neese, J. R. Long, *Nat. Chem.* **2013**, *5*, 577; h) S. Gomez-Coca, E. Cremades, N. Aliaga-Alcalde, E. Ruiz, *J. Am. Chem. Soc.* **2013**, *135*, 7010; i) Y.-Y. Zhu, C. Cui, Y.-Q. Zhang, J.-H. Jia, X. Guo, C. Gao, K. Qian, S.-D. Jiang, B.-W. Wang, Z.-M. Wang, S. Gao, *Chem. Sci.* **2013**, *4*, 1802; j) J. M. Zadrozny, M. Atanasov, A. M. Bryan, C.-Y. Lin, B. D. Rekken, P. P. Power, F. Neese, J. R. Long, *Chem. Sci.* **2013**, *4*, 125.

[8] a) A. V. Palii, B. S. Tsukerblat, E. Coronado, J. M. Clemente-Juan, J. J. Borras-Almenar, *J. Chem. Phys.* **2003**, *118*, 5566; b) A. V. Palii, B. S. Tsukerblat, E. Coronado, J. M. Clemente-Juan, J. J. Borrás-Almenar, *Inorg. Chem.* **2003**, *42*, 2455; c) F. Lloret, M. Julve, J. Cano, R. Ruiz-Garcia, E. Pardo, *Inorg. Chim. Acta* **2008**, *361*, 3432.

[9] a) M. Mikuriya, M. Fukuya, *Chem. Lett.* **1998**, 421; b) B. Chiari, A. Cinti, O. Crispu, F. Demartin, A. Pasini, O. Piovesana, *J. Chem. Soc., Dalton Trans.* **2002**, *5*, 4672; c) A. Ferguson, A. Parkin, J. Sanchez-Benitez, K. Kamenev, W. Wersndorfer, M. Murrie, *Chem. Commun.* **2007**, 3473; d) T. C. Stamatatos, A. K. Boudalis, K. V. Pringouri, C. P. Raptopoulou, A. Terzis, J. Wolowska, E. J. L. McInnes, S. P. Perlepes, *Eur. J. Inorg. Chem.* **2007**, *32*, 5098; e) L. F. Chibotaru, L. Ungur, C. Aronica, H. Elmoll, G. Pilet, D. Luneau, *J. Am. Chem. Soc.* **2008**, *130*, 12445; f) P. Alborés, E. Rentschler, *Angew. Chem. Int. Ed.* **2009**, *48*, 9366; *Angew. Chem.* **2009**, *121*, 9530; g) Z.-Q. Jia, X.-J. Sun, L.-L. Hu, J. Tao, R. B. Huang, L. S. Zheng, *Dalton Trans.* **2009**, 6364; h) V. Tudor, A. Madalan, V. Lupu, F. Lloret, M. Julve, M. Andruh, *Inorg. Chim. Acta* **2010**, *363*, 823; i) I. C. Lazzarini, L. M. Carrella, E. Rentschler, P. Alborés, *Polyhedron* **2012**, *31*, 779; j) A. A. Kitos, C. G. Efthymiou, C. Papatriantafyllopoulou, V. Nastopoulos, A. J. Tasiopoulos, M. J. Manos, W. Wersndorfer, G. Christou, S. P. Perlepes, *Polyhedron* **2011**, *30*, 2987; k) S.-Y. Y. Zhang, B. Xu, L. N. Zheng, W. Q. Chen, Y. H. Li, W. Li, *Inorg. Chim. Acta* **2011**, *367*, 44; l) S. Banerjee, M. Nandy, S. Sen, S. Mandal, G. M. Rosair, A. M. Z. Slawin, C. J. G. Garcia, J. M. Clemente-Juan, E. Zangrando, N. Guidoling, S. Mitra, *Dalton Trans.* **2011**, 1652; m) L. N. Saunders, M. E. Pratt, S. E. Hann, L. N. Dawe, A. Decken, F. M. Kerton, C. M. Kozak, *Polyhedron* **2012**, *46*, 53; n) D. Wu, X. Zhang, P. Huang, W. Huang, M. Ruan, Z. W. Ouyang, *Inorg. Chem.* **2013**, *52*, 10976; o) S. R. Hosseinian, V. Tangoulis, M. Menelaou, C. P. Raptopoulou, V. Psycharis, C. Dendrinou-Samara, *Dalton Trans.* **2013**, *42*, 5355; p) T. Roy Barman, M. Sutradhar, M. G. B. Drew, E. Rentschler, *Polyhedron* **2013**, *51*, 192; q) P. Mondal, R. Singh, A. Hens, J. Cano, E. Colacio, K. K. Rajak, *Polyhedron* **2013**, *65*, 60.

[10] C. Redshaw, M. R. J. Elsegood, J. W. A. Frese, S. Ashby, Y. Chao, A. Mueller, *Chem. Commun.* **2012**, *48*, 6627.

[11] a) W.-G. Lu, C.-H. Peng, H.-W. Liu, X.-L. Feng, *Chin. J. Inorg. Chem.* **2003**, *19*, 1222; b) A. Rotondo, G. Bruno, G. Brancatelli, F. Nicolo, D. Armentano, *Inorg. Chim. Acta* **2009**, *362*, 247.

[12] a) P. Alborés, E. Rentschler, *Dalton Trans.* **2009**, *2*, 2609; b) G. Aromi, A. S. Batsanov, P. Christian, M. Helliwell, A. Parkin, S. Parsons, A. A. Smith, G. A. Timco, R. E. P. Winpenny, *Chem. Eur. J.* **2003**, *9*, 5142.

[13] U. Englert, J. Strahle, *Z. Naturforsch. B* **1987**, *42*, 959.

[14] M. E. Lines, *J. Chem. Phys.* **1971**, *55*, 2977.

[15] S. Alvarez, P. Alemany, D. Casanova, J. Cirera, M. Llunell, D. Avnir, *Coord. Chem. Rev.* **2005**, *249*, 1693.

[16] O. Kahn, *Molecular Magnetism*, VCH Publishers, New York, **1993**.

[17] a) A. Abraham, B. Bleaney, *Electron Paramagnetic Resonance of Transition Ions*, Oxford University Press, **1970**; b) L. Banci, A. Bencini, C. Benelli, D. Gatteschi, C. Zanchini, *Struct. Bonding (Berlin)* **1982**, *52*, 37.

[18] a) A. B. Boeer, A.-L. L. Barra, L. F. Chibotaru, D. Collison, E. J. L. McInnes, R. A. Mole, G. G. Simeoni, G. A. Timco, L. Ungur, T. Unruh, R. E. P. Winpenny, *Angew. Chem. Int. Ed.* **2011**, *50*, 4007; *Angew. Chem.* **2011**, *123*, 4093; b) F. Habib, O. R. Luca, V. Vieru, M. Shiddiq, I. Korobkov, S. I. Gorelsky, M. K. Takase, L. F. Chibotaru, S. Hill, R. H. Crabtree, M. Murugesu, *Angew. Chem. Int. Ed.* **2013**, *52*, 1; c) J. J. Liu, S. Datta, E. Bolin, J. Lawrence, C. C. Beedle, E. C. Yang, P. Goy, D. N. Hendrickson, S. Hill, *Polyhedron* **2009**, *28*, 1922.

[19] a) P. Alborés, C. Plenk, E. Rentschler, *Inorg. Chem.* **2012**, *51*, 8373; b) P. Alborés, E. Rentschler, *Dalton Trans.* **2010**, 5005; c) P. Alborés, E. Rentschler, *Inorg. Chem.* **2010**, *49*, 8953; d) P. Alborés, E. Rentschler, *Eur. J. Inorg. Chem.* **2008**, 4004; e) P. Alborés, J. Seeman, E. Rentschler, *Dalton Trans.* **2009**, 7660; f) P. Alborés, E. Rentschler, *Inorg. Chem.* **2008**, *47*, 7960.

[20] a) V. Tudor, A. Madalan, V. Lupu, F. Lloret, M. Julve, M. Andruh, *Inorg. Chim. Acta* **2010**, *363*, 823; b) M. Moragues-Canovas, C. E. Talbot-Eeckelaers, L. Catala, F. Lloret, W. Wersndorfer, E. K. Brechin, T. Mallah, *Inorg. Chem.* **2006**, *45*, 7038; c) L.-L. L. Hu, Z.-Q. Q. Jia, J. Tao, R.-B. B. Huang, L. S. Zheng, *Dalton Trans.* **2008**, 6113; d) A. Ferguson, M. Schmidtmann, E. K. Brechin, M. Murrie, *Dalton Trans.* **2011**, *40*, 334; e) T. Shiga, H. Oshio, *Polyhedron* **2007**, *26*, 1881.

[21] S. Akine, T. Taniguchi, T. Nabeshima, *Inorg. Chem.* **2008**, *47*, 3255.

[22] S. Stoll, A. Schweiger, *J. Magn. Reson.* **2006**, *178*, 42.

[23] *SCALE3 ABSPACK: Empirical absorption correction*, CrysAlis – Software package, Oxford Diffraction Ltd., Oxford, UK, **2006**.

[24] *SHELXS97 and SHELXL97*, *Programs for Crystal Structure Resolution*, G. M. Sheldrick, University of Göttingen, Germany, **1997**.

[25] G. te Velde, F. M. Bickelhaupt, E. J. Baerends, C. Fonseca Guerra, S. J. A. van Gisbergen, J. G. Snijders, T. Ziegler, *J. Comput. Chem.* **2001**, *22*, 931.

[26] L. Noodleman, *J. Chem. Phys.* **1981**, *74*, 5737.

[27] L. Noodleman, E. J. Baerends, *J. Am. Chem. Soc.* **1984**, *106*, 2316.

[28] E. Ruiz, J. Cano, S. Alvarez, P. Alemany, *J. Comput. Chem.* **1999**, *20*, 1391.

[29] F. Neese, *J. Phys. Chem. Solids* **2004**, *65*, 781.

Received: February 20, 2014
Published Online: April 11, 2014

 © 2014 Wiley-VCH Verlag GmbH & Co. KGaA, Weinheim